Reaktor

p-ISSN 0852 – 0798
e-ISSN 2407 – 5973

Website: http://ejournal.undip.ac.id/index.php/reaktor/

Reaktor, Vol. 22 No. 2, August Year 2022, pp. 49-58

Cellulose Nanofibers Derived from Cigarette Butts Deacetylation and Its Application in Pickering Emulsion

Putri Amanda*[1], Nanang Masruchin[1] and Anita Amelia[2]

[1]Research Center for Biomass and Bioproduct, National Research and Innovation Agency, Cibinong Science Center, Jl. Raya Bogor KM 46, Cibinong, 16911, Indonesia
[2]Environmental and Industrial Hygiene Division, PETROLAB Services, PT Pisangan Lama 3 Street No.28, Jakarta, 13230, Indonesia

*) Corresponding author: putri.amanda@brin.go.id

(Received: 16 May 2022; Published: 18 August 2022)

Abstract

Cellulose nanofibers (CNF) have been applied in various applications due to the abundant raw materials and excellent mechanical and thermal properties. In this work, CNF from Cigarette butts (CNF-CB) was used as emulsion stabilized for oil in water emulsion. CNF was prepared from regenerated cellulose fibers produced by alkaline autoclaving deacetylation at 121°C for 15 minutes and then Acid hydrolysis using 55 wt.% of sulfuric acids at 45 ◦C for 45 min. The FTIR spectra of CNF-CB showed chemically convert from Cigarette butts waste, indicating removal of the acetyl group. TEM micrographs showed nanocellulose with diameters of 8-32.30 nm. XRD analysis showed that the CNF-CB is a cellulose II allomorph with a crystallinity index of about 88.04%. Thermogravimetric analysis showed high char residue for the nanocellulose compared to raw fibers. The addition of CNF-CB with a concentration of 0.5% into the oil-in-water emulsion (O/W) showed better stability than commercial surfactant. In conclusion, this approach offers a promising strategy for upcycling cigarette butts waste to produce nanocellulose, which could be used in various applications.

Keywords: *Deacetylation, Acid hydrolysis, Cigarette Butts, Cellulose Nanofibers, Pickering emulsion*

How to Cite This Article: Amanda, P., Masruchin, N., & Amelia, A. (2022). Cellulose Nanofibers from Regenerated Cellulose fibers of Cigarette Butts and Application in Pickering Emulsion. Reaktor, 22(2). 49-58 https://doi.org/10.14710/reaktor.22.2.49-58

INTRODUCTION

Pickering emulsion is an emulsion that uses solid particles as an alternative surfactant to improve the emulsification process and emulsion stability. (Albert et al., 2019; Chevalier & Bolzinger, 2013; Z. Sun et al., 2022). For several decades, Pickering emulsion has been applied in various of applications, from drug delivery and pharmaceutics to cosmetics and the food industry (Saffarionpour, 2020). Numerous solid particle is used in Pickering emulsions, such as silica particles (Macedo Fernandes Barros et al., 2019; Tikekar et al., 2013), mineral particles (Teixeira et al., 2011), metal oxide (Zhai et al., 2013), polymer particles, and even biopolymer such as nanocellulose (Aaen et al., 2019; Asabuwa Ngwabebhoh et al., 2018; Salas et al., 2014).

Nowadays, nanocellulose as a biobased material has sparked much attention and scientific curiosity in research and development (Reubroycharoen et al., 2018; Shaghaleh et al., 2018). During the past decade, nanocellulose was generally extracted from lignocellulosic biomass, bacterial cellulose, or natural fibers (Li et al., 2018; Valencia et al., 2019). However, the limitation of the forest and agriculture sectors for cellulose resources makes non-plant cellulosic sources getting worldwide interest and attention. Utilization of discarded waste such as Cigarette butts to produce nanocellulose is a great

challenge that we can do to tackle the problem of unbalancing natural processes and waste disposal.

As one of the highest smoking rates globally, Indonesia is also one of the largest tobacco manufacturers in the world. Indonesia's cigarette consumption more than doubled (from 136 to 293 billion cigarettes) between 1995-2013 (Suprihanti et al., 2018). In 2020, the Statista Research Department showed that approximately 261.4 thousand metric tons of tobacco produced in Indonesia with the favored form of tobacco product there are "kretek," and the production of this "kretek" expect to continue to increase in line with the growing population of Indonesia (www.statista.com). In 2017, in the book Tobacco and Its Environmental Impact, WHO reported that one cigarette butt contains more than 7000 toxic chemicals (WHO, 2017). In 2011, researchers from the Suffrinder foundation found that one cigarette butt in one liter of water was enough to kill half the fish used in the study. Furthermore, Nicotine levels in water exceeding the threshold have been reported in Berlin, Germany, where accumulations increased from 2.5 to 3.8 mg/L from the dry to the rainy season. (Roder Green et al., 2014)

Cigarette butts are materials conducted with cellulose acetate as the main component with plasticizer addition as a binder, and it takes a long time to decompose in nature. Ogundare et al. (2017) reported that it takes 2-10 years for cellulose acetate from cigarette butts to decompose. It only breaks into smaller sizes, which detaches into the environment in the form of microplastics. (Ogundare et al., 2017)

Cellulose acetate results from a reaction of cellulose acetylation with Anhydrous Acetate and Acetic Acid with Sulfuric Acid (Duan & Yu, 2016; S. Nair & Mathew, 2017; Yu et al., 2017). The removal of acetyl clusters can be performed known as deacetylation reactions. Deacetylation of cellulose acetate can produce cellulose that is easily decomposed in nature and can be used for further applications such as to produce nanocellulose.

The principle of the preparation of nanocellulose is to break hydrogen bonds in cellulose chains. Mechanical fibrillation has been successfully used in producing cellulose nanofibers using milling (Phanthong et al., 2016; Piras et al., 2019; Zheng et al., 2018), grinding (P. Amanda et al., 2021; Syafri et al., 2022; Q. Q. Wang et al., 2012), high-pressure homogenizer (J. A. Lee et al., 2014), and microfluidizer (J. Wang et al., 2021). However, very intensive energy is needed in the mechanical fibrillation process.

Nanocellulose isolation from cigarette butts had previously been conducted by Ogundare et al. in 2017 with deacetylation of cigarette butts using conventional methods by immersion with Ethanolic-NaOH solution. Our previous research successfully converts cellulose acetate in cigarette butts to regenerated cellulose fibers faster and easier using NaOH and autoclave for 15 minutes with a percentage of deacetylation degrees of 87.19% (Amanda et al., 2020).

This work aimed to isolate and characterize nanocellulose from autoclave-assisted deacetylation of cigarette butts. Thermal stability, shape, and crystallinity are all aspects of nanocellulose characterization. After that, nanocellulose is utilized as a stabilizer in sunflower oil emulsions. Sunflower oil contains Vitamin E and can absorb UVB rays, which makes it worthwhile as one of the most used ingredients in the cosmetic industry, such as sunscreen. Among all the different types of cosmetics products, an emulsion is one of the most products found in the market.

The results of this research were expected to provide information on the management of cellulose acetate waste from cigarette butts into new materials with added value, such as nanocellulose. Furthermore, the information about Pickering emulsion characteristics could be the initial information for using CNF-CB as a Pickering agent for a more comprehensive application in cosmetics and other industries.

MATERIAL AND METHOD

Material

Cigarette butts were collected at the Cibinong Science Center- Botanical Garden (CSC-BG), Cibinong, Bogor. NaOH (reagent grade, ≥98%, pellets), Sulfuric Acid (98%), Sodium Chloride, Ethanol (99,8%), and NaOCl (reagent grade with chlorine content 12%) were purchased from Sigma Aldrich. All chemicals were used as received without other purification**.**

Preparation of Cigarettes Butts

The filters were first manually separated from paper and tobacco. Filters (ca. 10 g) were then soaked and washed with water, drained, and extracted with ethanol (20 mL/g) for 24 h at room temperature. After extraction, the obtained cellulose acetate (CA-CB) was bleached using 1.25 w/v% NaOCl (10 mL/g) for 6 h at room temperature.(Ogundare et al., 2017)

Extraction of Cellulose from Cigarettes butts

Regenerated cellulose fibers (RCF) were extracted from cellulose acetate of CB using our previous method, by autoclaved assisted using NaOH (0.25 M,(20 mL/g) for 15 min at the temperatures of 121°C (Amanda et al., 2020). After deacetylated process, RCF washed with aquadest until the pH was 7.

Isolation of Cellulose Nanofibers

Cellulose Nanofiber from CB (CNF-CB) was isolated from RCF via acid hydrolysis using method that reported by Ogundare., 20 mL/g (volume acid per mass of cellulose) of 55 wt.% sulfuric acids at 45 ◦C in an oil bath for 45 min to remove the amorphous regions of RCF (Ogundare et al., 2017). Following the acid hydrolysis, the suspension diluted 20 times its initial volume with double distilled water at room

temperature and centrifuged using Tomy High-Speed Refrigerated Centrifuge at 10.000 rpm for 10 min. This process was repeated several times to reduce the sulfuric acid concentration. After neutralization pH, the suspensions were then sonicated using an ultrasonicated (Omni Sonic Ruptor 400 Ultrasonic homogenizer, Georgia) at 40% amplitude for 15 min to ensure complete CNF-CB dispersion and avoid aggregation.

CNF-CB suspension was rapidly frozen refrigerator overnight and freeze-dried for 72 h at −60 ◦C in a Labconco FreeZone for future characterization. The percent-age yield of the isolated CNC was determined gravimetrically as shown in Equation (1):

$$\%\ Yield\ of\ CNF-CB = \frac{\text{weight of CNF–CB isolated } (g)}{Weight\ of\ Cel-CB\ \ used\ (g)}\ x\ 100\% \qquad (1)$$

Characterization of Nanocellulose

Various properties of RCF and CNF were evaluated in various characterizations. Fourier transform infrared (FT-IR) spectra of every sample were obtained utilizing a FTIR spectrometer Spectrum Two, equipped with universal diamond crystal attenuated total reflection (ATR) accessory (Perkin Elmer, USA) to collect detailed information of the functional groups of the freeze-dried samples after chemical treatments. The spectra were recorded in the range of 500–4000 cm^{-1} with a resolution of 4 cm^{-1}.

The morphological transition of CB to CNF-CB was analyzed by Field Emission Scanning Electron Microscope (FESEM) and Transmission Electron Microscope (TEM), respectively. TEM images of the CNF-CB sample were acquired using 0.1 w/w% suspension of CNF-CB using TEM JEOL 1010 (80.0KV, Magnification 50.000x). The dimensions of 100 spot randomly selected representative CNF-CB from the TEM micrographs were measured using ImageJ 1.42 software and the obtained data were processed on OriginPro 8 software. For the SEM study of CB, the FESEM- Quatro S was used. The acceleration voltage was set at 1 kV.

The crystallinity CB, RCF and CNF-CB was determined by using X-ray diffractometer (XRD-7000, Shimadzu, Japan) equipped with a Cu-Kα radiation source (wavelength = 0.154 nm) operating at 40 kV and 30 mA. The XRD pattern was recorded over the angular range 5° to 50° at room temperature. The crystallinity index (CrI) was calculated using Segal's method (Nam et al., 2016; Segal et al., 1959), as shown in Equation (2).

$$CI = \frac{I_{002} - I_{AM}}{I_{002}} \qquad (2)$$

where I_{200} signifies amorphous and crystalline fractions and IAM signifies amorphous region.

The thermal analyses were conducted using thermogravimetric analyzer (TGA, Perkin Elmer 4000). All samples were heated from 25 ºC to 500 ºC under Nitrogen atmosphere at a heating rate of 10 ºC/min.

Pickering Emulsion Preparation

Oil-in-water (o/w) emulsions were prepared using disperser ultraturax IKA T25 (IKA works, Wilmington NC) for two minutes operating at 8000rpm. Sunflower oil was selected as model oil. Emulsions with 10% oil (by volume) were prepared in a 30 mL glass vial. After preparation, emulsions were immediately poured into cylindrical sample bottles and their stability was investigated by recording the change in height with time of the emulsion-aqueous phase interface and then evaluating the volume fraction changes of the stable emulsion and resolved water.

Zeta potential of the emulsion droplets was measured using a Zetasizer (Model: Malvern Nano Series, Malvern Instruments, Inc., Westborough, MA), and 3D microscope viewed using an optical microscope Keyence VHX600 fit digital camera. The mean droplet diameter was measured using ImageJ and origin software.

RESULTS AND DISCUSSION

Cellulose Nanofibers Yield

Nanocellulose was isolated from CB after extraction, bleaching, autoclave-assisted deacetylation, and acid hydrolysis Cellulose of RCF with sulfuric acid. Nanocellulose was isolated from CB after extraction, bleaching, autoclave-assisted deacetylation, and acid hydrolysis Cellulose of RCF with sulfuric acid. Chemical isolation via acid hydrolysis is a popular approach for producing nanocrystalline cellulose. One advantage of acid isolation is the abundance of hydroxyl groups in nanocellulose. It makes nanocellulose highly reactive and hydrophilic, allowing mixing and dispersion in various matrices (Sartika et al., 2019). In this research, we hydrolysis the RCF following the research of Ogundare et al. 2017 who has done acid hydrolysis of discarded cigarette butts before.

The yield obtained RCF from CB was 87%, this result inline with RCF that result from wood fibers/PP composites by Lee et.al in 2013 (S. Lee et al., 2014) which about 70-90%. Furthermore, The CNF-CB from RCF was 42.4%. This result is lower than CNF which was obtained from plant resources such as CNF from bagasse using formic acid hydrolysis for three hours with yield of 74,66% (Sri Aprilia et al., 2017). However, this study showed significant cellulose nanofiber production compared to the results reported by Schoeler et.al., which was isolated nanocellulose from chemically purified cellulose (CPC) of Cassava Agro-industrial Waste (CAW) with 9% of yield (Schoeler et al., 2020). There are various parameters which affected the yield of nanocellulose such as type of raw material, chemical composition of raw material and parameters of hydrolysis process (P. Amanda et al., 2021; Masruchin et al., 2020).

Characterization of Cellulose Nanofibers

FTIR Spectroscopy Analysis

The FTIR Spectroscopy confirmed CB's successful conversion to RCF, shown by the absence of acetyl peaks at 1733 cm^{-1} and 1215 cm^{-1} in the spectra, which indicates that cellulose acetate in CB is converted during the autoclaved deacetylation process.

The FTIR analysis shows that both RCF and CNF-CB obtained after acid hydrolysis treatment have the same basic structure, as shown in Figure 1. During the conversion of macro cellulose to nano-scale cellulose, the differences were controlled by changes in the hydroxyl group (Morán et al., 2008). The broad peak in the range 3352-3405 cm^{-1} for all samples is identified due to -OH stretching vibration (Kang et al., 2017; Supian et al., 2020). The -OH peak of the isolated CNF-CB showed identical absorption bands compared to the FTIR spectrum of RCF but with greater intensities. The intensification of these peaks indicated an increase in crystallinity due to the loss of the amorphous regions after acid hydrolysis (Al-Dulaimi & Wanrosli, 2017; Y. Sun et al., 2008)

The C–H stretching vibration and –CH2–(C6)– bending vibration peaks are around 2,886 and 1373 cm^{-1}. Cellulose-water interaction, which gives -OH bending of absorbed water, is also observed at 1641 cm-1. The peak of C-H_{asym} bending was shown at 1019 cm^{-1} (C-O-C) and 903 cm^{-1} (C-H_{deform}) modes of the β-glycosidic linkage between the anhydrous glucose rings (Al-Dulaimi & Wanrosli, 2017; Putri Amanda et al., 2020; Y. Sun et al., 2008).

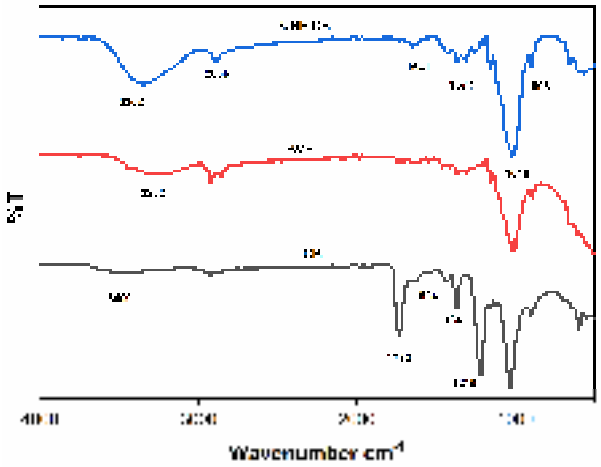

Figure 1. Fourier Transform Infrared (FTIR) spectra of CB, RCF, and CNF-CB

Morphology of Cellulose nanofibers

Figure 2 shows the SEM image of cellulose from cigarette butts with magnifications 163x. The surface morphology of RCF through SEM micrographs in Figure 2 presents the structure of long coarse fibril bundles with an average diameter of ±20 µm. Figure 3 shows the observations of TEM image CNF-CB resulting from acid hydrolysis treatment. This result indicated that CNFs displayed a fibrous network structure.

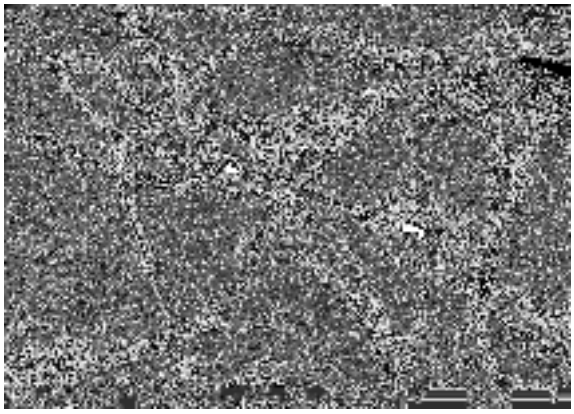

Figure 2. SEM images of Cigarette butt

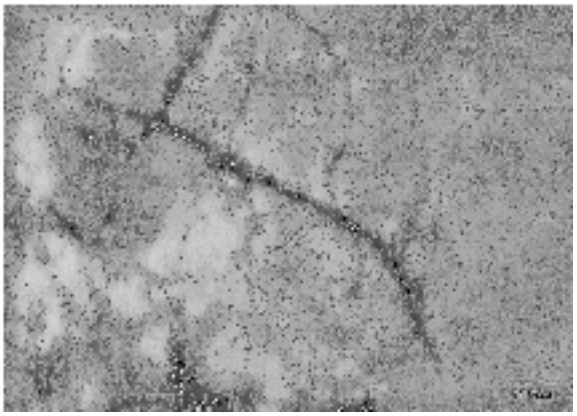

Figure 3. TEM images of CNF-CB

The structural morphology od CNF showed a high specific surface area compared to RCF from Cigarette butt. Based on TEM analysis, the diameter size of CNF-CB ranges from 8 to 32.30 ± 1.12 nm, which is higher than the CNFs diameter from Napier fiber (5.67-13.70 nm) which was obtained from ball mill assisted acid hydrolysis with 5.6 M sulfuric acid concentration and the CNFs from discarded crop straw show diameter 5-10 nm (Miao et al., 2020). It is important to note that the length of the obtained CNFs was estimated to be in the microscale.

XRD Analysis

Various techniques, including solid-state 13C NMR, Raman Spectroscopy, IR spectroscopy, and XRD, can be used to measure the crystallinity Index (CrI) of celluloses (Agarwal, 2017; Dufresne, 2017; Foster et al., 2018; Nam et al., 2016). Method using FTIR spectroscopy determines CrI by measuring relative peak heights or area. This technique is the simplest method but gives only relative values because the spectrum always contains a contribution from crystalline and amorphous regions. In this study, the crystalline structure of CNF-CB was identified by their characteristic X-ray diffraction pattern. Various methods have been used to calculate CrI from raw XRD data. The ratio between the intensity of the crystalline peak (I_{002}-I_{AM}) and total intensity (I_{002}) after

subtraction the signal of the background measured without cellulose can calculate the CrI of CNFs. Segal and a co-worker developed this method .(Nam et al., 2016)

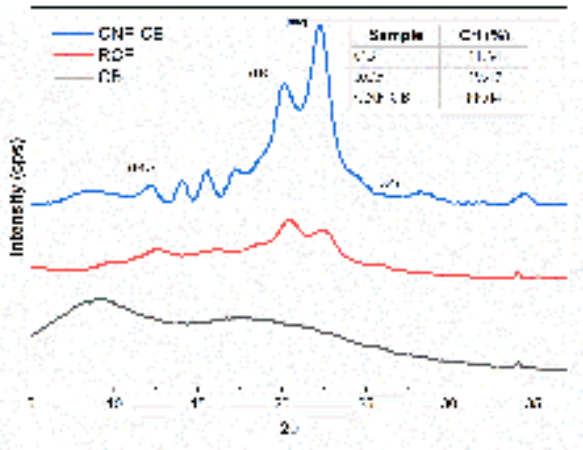

Figure 4. X-Ray Diffraction pattern of CB. RCF and CNF-CB

The XRD pattern of All samples is shown in Figure 4. The XRD pattern looks broad and low in RCF. In addition, at CB peak is obtained a broad peak at 2θ 20º, which indicates a high amorphous region. Furthermore, the higher CrI value in RCF compared to CB indicates that part of the amorph is lost in the deacetylation process. After hydrolysis with acid in RCF, CNF-CB is obtained with higher crystallinity, 88.04%.

The diffractograms peak are typical of cellulose II allomorphs. These peaks are located at 2θ: 12º, 20º, 22º and 34º which correspond to the diffraction of (1-10), (101), (002) and (004) crystallographic plane reflection respectively.(Ago et al., 2007; Gong et al., 2017; Han et al., 2013) These observations are consistent with the literature studied was reported by Ogundare et.al 2017 which isolated CNC from discarded Cigarette filter with conventional NaOH deacetylation. The characteristic of cellulose II allomorphs was an indication of the influence of alkaline hydrolysis while autoclave assisted deacetylation of CB (Mansikkamäki et al., 2007; Ogundare et al., 2017). Furthermore, Oudiani et.al 2011, treatment Agave americana L. fiber with aqueous NaOH solution of a specific concentration (15 wt.%) causes the completely transformation of cellulose I into cellulose II within the crystalline domains (Oudiani et al., 2011)

The forms of cellulose that have been investigated the most are cellulose I and II. Generally, the intra-sheet bonds in the cellulose II lattice are the same as in the cellulose I lattice structure, but cellulose II is more stable than cellulose I because of the variety of inter-sheet hydrogen bonds that can form; this also may explain why cellulose I can be converted to cellulose II but not the other way around (Gong et al., 2017; H. Wang et al., 2014).

Thermogravimetric analysis (TGA) Analysis

The thermal behavior of CB, RCF, and CNF-CB (freeze-dried) were determined by TGA. The thermogram curves shown in Figure 5 revealed comparable but different rates of thermal degradation profiles. A similar thermal degradation mechanism is suggested, but it proceeded at different rates. Table 1 presents the decomposition stages, the corresponding characteristic temperatures, mass losses, and ashes left at 500 ºC. The mass loss observed in the range of temperature 40–110 ºC is attributed to the loss of absorbed moisture on the surface.

Table.1. Comparison of thermal analysis data for CB, RCF, and CNF-CB

Sample	T_i (ºC)	T_p (ºC)	T_f (ºC)	Mass loss at T_p (%)
CB	303.02	377	421.14	72.37
RCF	220	350	376	64.82
CNF-CB	213	287.33	374	55.38

T_i: Initial temperaturem, T_p: Peak temperature, T_f: Final temprature

The moisture content of RCF is higher than CB, which is 7.07% and 1,67% weight loss at 110 ºC, respectively. The increasing moisture content of RCF correlated well with the increasing hydroxyl group of RCF, which was observed in FTIR spectra (Figure 1). For CNF-CB, because of the removal of the amorphous region during hydrolysis, the moisture content was 2.32% which decreased from RCF.

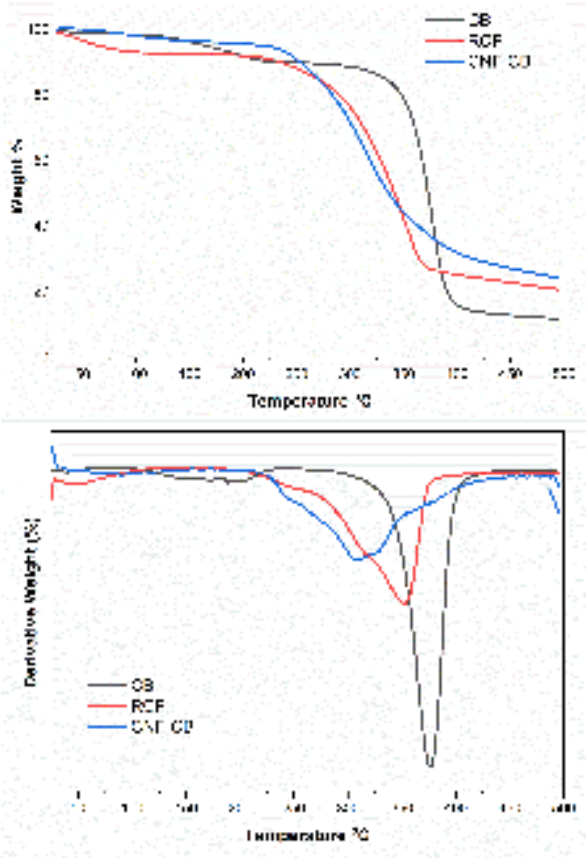

Figure 5. The thermogram of CB, RCF, and CNF-CB (a) TGA and (b) DTG

Cigarette butts showed the highest Tp at 377 ºC and the highest mass loss of 72.37%, and RCF showed Tp at 350 ºC and mass loss of 64.82%. In CNF-CB, the sulfate groups on freeze-dried CNF-CB samples reduce their thermal degradation. When released as sulfuric acid, it further catalyzed the degradation. It is evident from DTG peaks that the maximum temperature for CNF-CB showed the lowest peak temperature at 287.33 ºC. On the other hand, it is essential to add that CNF-CB has the lowest mass loss of 55.35% and high char residue of ca 25% compared with Cigarettes butts (ca. 10.7%); this is owing to the presence of sulfate groups in CNF which act as a flame retardant .(Thomas et al., 2021)

CNF-CB in Pickering Emulsion Application

Oil in water emulsions was prepared using sunflower oil as the oil phase and 0.5% of CNF-CB at fixed oil loading of 10% (v/v). The resultant emulsion stability against coalescence, creaming, and droplet size stability was evaluated over 30 days at room temperature.

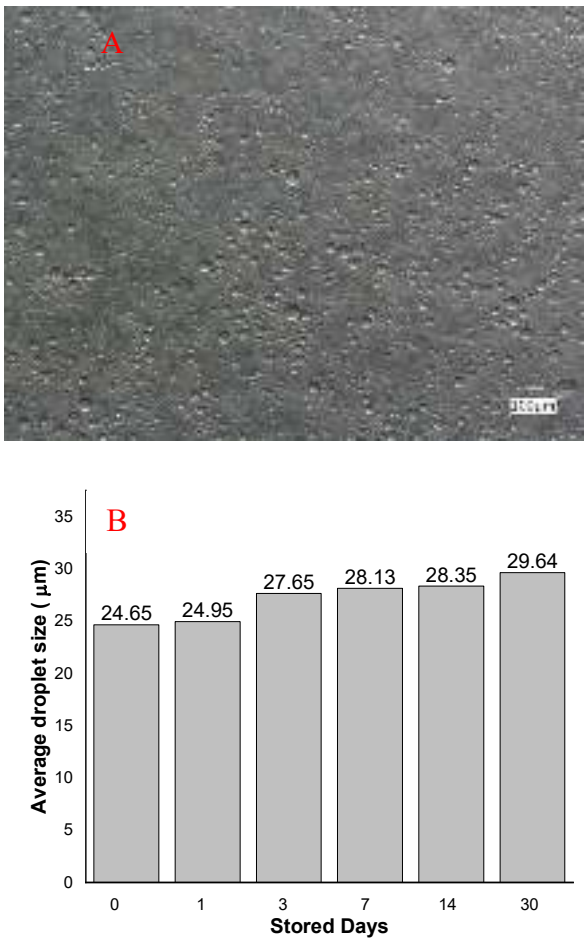

Figure 6. a) optical micrograph of emulsion 1h after preparation, b) the average droplet of emulsion in 30 days stored

The emulsion composed of the oil phase and CNF-CB were visualized using a 3D optical microscope, and the result is shown in Figure 6a. ImageJ measured the droplet sizes of emulsion with 200 sampling spots. The average droplet size of Pickering emulsions stabilized by CNF-CB on day 0, day 1, day 3, day 7, day 14, and day 30 were presented in Figure 7b. The emulsion exhibited good stability with a slight increase in droplet size throughout 30 days. The increase in average droplet sizes of CNF-CB-stabilized emulsions was primarily due to the coalescence of smaller unstable droplets into larger ones.

Furthermore, the fabricated CNF-CB stabilized emulsion was highly stable against creaming; no noticeable phase separation was observed, even after 30 days of storage. Meanwhile, the same emulsion system was obtained using a commercial surfactant, and the result shows emulsion separated after seven days stored. The improvement of the emulsification process and stabilization of the emulsion were mainly due to the amphiphilic properties of CNF-CB. Figure 7 shows the Comparison of Stability of the emulsion stabilized by CNF-CB, a commercial surfactant Tween 80, in 30 days stored.

Figure 7. Comparison of Stability the emulsion stabilized by CNF-CB a commercial surfactant in 30 days stored

These results demonstrated that CNF-CB could be an excellent stabilizer in forming Pickering emulsions of sunflower oil. The information about this Pickering emulsion can be the starting point for using CNF-CB as a Pickering agent in a broader application of sunflower oil emulsion, not only cosmetics but also other sectors.

CONCLUSION

Cellulose nanofibers from RCF of cigarette butts have been successfully isolated via Sulfuric acid hydrolysis. The chemical structure of the nanoparticles did not change during the acid hydrolysis process. The TEM study showed that CNF-CB were fibrils with mean diameters of 8-32.30 ± 1.12 nm. The CNF-CB forms a cellulose II allomorph with a crystallinity index of 88%. TGA results showed that CNF-CB has low thermal degradation but high thermal resistance. It could be attributed to the higher crystallinity of CNF-CB than RCF. Applications of CNF-CB in Pickering emulsion of Sunflower oil showed that the emulsion stabilized by CNF-CB had

better stability than commercial surfactant. The emulsion has a nanoscale size and exhibits only a slight increase in droplet size throughout 30 days of storage.

Finally, the results of this study reveal that these methods can be one the promising methods for upcycling Cigarette butt waste. As a Pickering agent, CNF-CB can be used not only for emulsion in cosmetic applications but also in other industries such as pharmaceutical, food packaging, or the oil industry.

AUTHORS' NOTE

The authors declares that there is no conflict of interest regarding the publication of this article. Authors confirmed that the data and the paper are free of plagiarism.

ACKNOWLEDGEMENT

All authors acknowledge the facilities, and the scientific and technical assistance of the Integrated Laboratory of Bioproducts at National Research and Innovation agency (BRIN).

REFERENCES

Aaen, R., Brodin, F. W., Simon, S., Heggset, E. B., & Syverud, K. (2019). Oil-in-water emulsions stabilized by cellulose nanofibrils—The effects of ionic strength and pH. *Nanomaterials*, *9*(2), 1–14. https://doi.org/10.3390/nano9020259

Agarwal, U. P. (2017). Raman Spectroscopy in the Analysis of Cellulose Nanomaterials. In *Nanocelluloses: Their Preparation, Properties, and Applications* (ACS Sympos, pp. 75–90). American Chemical Society. https://doi.org/10.1021/bk-2017-1251.ch004

Ago, M., Endo, T., & Okajima, K. (2007). Effect of Solvent on Morphological and Structural Change of Cellulose under Ball-Milling. *Polymer Journal*, *39*(5), 435–441. https://doi.org/10.1295/polymj.pj2006096

Al-Dulaimi, A. A., & Wanrosli, W. D. (2017). Isolation and Characterization of Nanocrystalline Cellulose from Totally Chlorine Free Oil Palm Empty Fruit Bunch Pulp. *Journal of Polymers and the Environment*, *25*(2), 192–202. https://doi.org/10.1007/s10924-016-0798-z

Albert, C., Beladjine, M., Tsapis, N., Fattal, E., Agnely, F., & Huang, N. (2019). Pickering emulsions: Preparation processes, key parameters governing their properties and potential for pharmaceutical applications. *Journal of Controlled Release*, *309*, 302–332. https://doi.org/10.1016/j.jconrel.2019.07.003

Amanda, P., Nabila, S., Qonita, N., Ningrum, R. S., Ismadi, & Masruchin, N. (2021). The Properties of OPEFB Cellulose Nanofibrils Produced by A Different Mode of Ultrafine Grinding. *IOP Conference Series: Earth and Environmental Science*, *891*(1), 012016. https://doi.org/10.1088/1755-1315/891/1/012016

Amanda, Putri, Putri, A., Masruchin, N., Kusumaningrum, W. B., & Ningrum, R. S. (2020). Autoclave-Assited Deactylation : A Rapid Method to Recycling Cigarette Butts Into Cellulose. *Jurnal Sains Materi Indonesia*, *22*(1).

Asabuwa Ngwabebhoh, F., Ilkar Erdagi, S., & Yildiz, U. (2018). Pickering emulsions stabilized nanocellulosic-based nanoparticles for coumarin and curcumin nanoencapsulations: In vitro release, anticancer and antimicrobial activities. *Carbohydrate Polymers*, *201*(June), 317–328. https://doi.org/10.1016/j.carbpol.2018.08.079

Chevalier, Y., & Bolzinger, M.-A. (2013). Emulsions stabilized with solid nanoparticles: Pickering emulsions. *Colloids and Surfaces A: Physicochemical and Engineering Aspects*, *439*, 23–34. https://doi.org/10.1016/j.colsurfa.2013.02.054

Duan, L., & Yu, W. (2016). Review of recent research in nano cellulose preparation and application from jute fibers. *Proceedings of the 2016 3rd International Conference on Materials Engineering, Manufacturing Technology and Control*, *37*(1–2), 20–28. https://doi.org/10.2991/icmemtc-16.2016.148

Dufresne, A. (2017). Handbook of Nanocellulose and Cellulose Nanocomposites. In *Handbook of Nanocellulose and Cellulose Nanocomposites*. https://doi.org/10.1002/9783527689972

Foster, E. J., Moon, R. J., Agarwal, U. P., Bortner, M. J., Bras, J., Camarero-Espinosa, S., Chan, K. J., Clift, M. J. D., Cranston, E. D., Eichhorn, S. J., Fox, D. M., Hamad, W. Y., Heux, L., Jean, B., Korey, M., Nieh, W., Ong, K. J., Reid, M. S., Renneckar, S., … Youngblood, J. (2018). Current characterization methods for cellulose nanomaterials. *Chemical Society Reviews*, *47*(8), 2609–2679. https://doi.org/10.1039/c6cs00895j

Gong, J., Li, J., Xu, J., Xiang, Z., & Mo, L. (2017). Research on cellulose nanocrystals produced from cellulose sources with various polymorphs. *RSC Advances*, *7*(53), 33486–33493. https://doi.org/10.1039/c7ra06222b

Han, J., Zhou, C., French, A. D., Han, G., & Wu, Q. (2013). Characterization of cellulose II nanoparticles regenerated from 1-butyl-3-methylimidazolium chloride. *Carbohydrate Polymers*, *94*(2), 773–781. https://doi.org/10.1016/j.carbpol.2013.02.003

Kang, X., Sun, P., Kuga, S., Wang, C., Zhao, Y., Wu, M., & Huang, Y. (2017). Thin Cellulose Nanofiber

from Corncob Cellulose and Its Performance in Transparent Nanopaper. *ACS Sustainable Chemistry and Engineering*, *5*(3), 2529–2534. https://doi.org/10.1021/acssuschemeng.6b02867

Lee, J. A., Yoon, M. J., Lee, E. S., Lim, D. Y., & Kim, K. Y. (2014). Preparation and characterization of cellulose nanofibers (CNFs) from microcrystalline cellulose (MCC) and CNF/polyamide 6 composites. *Macromolecular Research*, *22*(7), 738–745. https://doi.org/10.1007/s13233-014-2121-y

Lee, S., Pan, H., Hse, C. Y., Gunasekaran, A. R., & Shupe, T. F. (2014). Characteristics of regenerated nanocellulosic fibers from cellulose dissolution in aqueous solutions for wood fiber/polypropylene composites. *Journal of Thermoplastic Composite Materials*, *27*(4), 558–570. https://doi.org/10.1177/0892705713484739

Li, J., Cha, R., Mou, K., Zhao, X., Long, K., Luo, H., Zhou, F., & Jiang, X. (2018). Nanocellulose-Based Antibacterial Materials. *Advanced Healthcare Materials*, *7*(20), 1–16. https://doi.org/10.1002/adhm.201800334

Macedo Fernandes Barros, F., Chassenieux, C., Nicolai, T., de Souza Lima, M. M., & Benyahia, L. (2019). Effect of the hydrophobicity of fumed silica particles and the nature of oil on the structure and rheological behavior of Pickering emulsions. *Journal of Dispersion Science and Technology*, *40*(8), 1169–1178. https://doi.org/10.1080/01932691.2018.1500480

Mansikkamäki, P., Lahtinen, M., & Rissanen, K. (2007). The conversion from cellulose I to cellulose II in NaOH mercerization performed in alcohol-water systems: An X-ray powder diffraction study. *Carbohydrate Polymers*, *68*(1), 35–43. https://doi.org/10.1016/j.carbpol.2006.07.010

Masruchin, N., Amanda, P., Kusumaningrum, W. B., Suryanegara, L., & Nuryawan, A. (2020). Particle Size Distribution and Yield Analysis of Different Charged Cellulose Nanofibrils Obtained by TEMPO-mediated Oxidation. *IOP Conference Series: Earth and Environmental Science*, *572*(1), 012045. https://doi.org/10.1088/1755-1315/572/1/012045

Miao, X., Lin, J., & Bian, F. (2020). Utilization of discarded crop straw to produce cellulose nanofibrils and their assemblies. *Journal of Bioresources and Bioproducts*, *5*(1), 26–36. https://doi.org/10.1016/j.jobab.2020.03.003

Morán, J. I., Alvarez, V. A., Cyras, V. P., & Vázquez, A. (2008). Extraction of cellulose and preparation of nanocellulose from sisal fibers. *Cellulose*, *15*(1), 149–159. https://doi.org/10.1007/s10570-007-9145-9

Nam, S., French, A. D., Condon, B. D., & Concha, M. (2016). Segal crystallinity index revisited by the simulation of X-ray diffraction patterns of cotton cellulose Iβ and cellulose II. *Carbohydrate Polymers*, *135*, 1–9. https://doi.org/10.1016/j.carbpol.2015.08.035

Ogundare, S. A., Moodley, V., & van Zyl, W. E. (2017). Nanocrystalline cellulose isolated from discarded cigarette filters. *Carbohydrate Polymers*, *175*, 273–281. https://doi.org/10.1016/j.carbpol.2017.08.008

Oudiani, A. El, Chaabouni, Y., Msahli, S., & Sakli, F. (2011). Crystal transition from cellulose i to cellulose II in NaOH treated Agave americana L. fibre. *Carbohydrate Polymers*, *86*(3), 1221–1229. https://doi.org/10.1016/j.carbpol.2011.06.037

Phanthong, P., Guan, G., Ma, Y., Hao, X., & Abudula, A. (2016). Effect of ball milling on the production of nanocellulose using mild acid hydrolysis method. *Journal of the Taiwan Institute of Chemical Engineers*, *60*, 617–622. https://doi.org/10.1016/j.jtice.2015.11.001

Piras, C. C., Fernández-Prieto, S., & De Borggraeve, W. M. (2019). Ball milling: a green technology for the preparation and functionalisation of nanocellulose derivatives. *Nanoscale Advances*, *1*(3), 937–947. https://doi.org/10.1039/C8NA00238J

Reubroycharoen, P., Phanthong, P., Abudula, A., Hao, X., Xu, G., & Guan, G. (2018). Nanocellulose: Extraction and application. *Carbon Resources Conversion*, *1*(1), 32–43. https://doi.org/10.1016/j.crcon.2018.05.004

Roder Green, A. L., Putschew, A., & Nehls, T. (2014). Littered cigarette butts as a source of nicotine in urban waters. *Journal of Hydrology*, *519*(PD), 3466–3474. https://doi.org/10.1016/j.jhydrol.2014.05.046

S. Nair, S., & Mathew, A. P. (2017). Porous composite membranes based on cellulose acetate and cellulose nanocrystals via electrospinning and electrospraying. *Carbohydrate Polymers*, *175*, 149–157. https://doi.org/10.1016/j.carbpol.2017.07.048

Saffarionpour, S. (2020). Nanocellulose for Stabilization of Pickering Emulsions and Delivery of Nutraceuticals and Its Interfacial Adsorption Mechanism. *Food and Bioprocess Technology*, *13*(8), 1292–1328. https://doi.org/10.1007/s11947-020-02481-2

Salas, C., Nypelö, T., Rodriguez-Abreu, C., Carrillo, C., & Rojas, O. J. (2014). Nanocellulose properties and applications in colloids and interfaces. *Current Opinion in Colloid and Interface Science*, *19*(5), 383–

396. https://doi.org/10.1016/j.cocis.2014.10.003

Sartika, D., Syamsu, K., Warsiki, E., & Fahma, F. (2019). Optimization of Sulfuric Acid Concentration and Hydrolysis Time on Crystallinity of Nanocrystalline Cellulose: A Response Surface Methodology Study. *IOP Conference Series: Earth and Environmental Science*, *355*(1). https://doi.org/10.1088/1755-1315/355/1/012109

Schoeler, M. N., Scremin, F. R., de Mendonça, N. F., Benetti, V. P., de Jesus, J. A., de Oliveira Basso, R. L., & Stival Bittencour, P. R. (2020). Cellulose Nanofibers from Cassava Agro-Industrial Waste as Reinforcement in Pva Films. *Quimica Nova*, *43*(6), 711–717. https://doi.org/10.21577/0100-4042.20170542

Segal, L., Creely, J. J., Martin, A. E., & Conrad, C. M. (1959). An Empirical Method for Estimating the Degree of Crystallinity of Native Cellulose Using the X-Ray Diffractometer. *Textile Research Journal*, *29*(10), 786–794. https://doi.org/10.1177/004051755902901003

Shaghaleh, H., Xu, X., & Wang, S. (2018). Current progress in production of biopolymeric materials based on cellulose, cellulose nanofibers, and cellulose derivatives. In *RSC Advances* (Vol. 8, Issue 2, pp. 825–842). Royal Society of Chemistry. https://doi.org/10.1039/c7ra11157f

Sri Aprilia, N. A., Chintia Ambarita, A., Karmila, K., Adam Armando, M., & Yusupi Guswara, F. (2017). Isolation and Characterization of Cellulose Nanofiber (CNF) from Sugarcane Bagasse by Acid Hydrolysis with Addition of Ferric Chloride Catalyst (FeCl3). *Oriental Journal of Physical Sciences*, *2*(2), 103–108. https://doi.org/10.13005/ojps02.02.09

Sun, Y., Lin, L., Deng, H., Li, J., He, B., Sun, R., & Ouyang, P. (2008). Structural changes of bamboo cellulose in formic acid. *BioResources*, *3*(2), 297–315. https://doi.org/10.15376/biores.3.2.297-315

Sun, Z., Yan, X., Xiao, Y., Hu, L., Eggersdorfer, M., Chen, D., Yang, Z., & Weitz, D. A. (2022). Pickering emulsions stabilized by colloidal surfactants: Role of solid particles. *Particuology*, *64*, 153–163. https://doi.org/10.1016/j.partic.2021.06.004

Supian, M. A. F., Amin, K. N. M., Jamari, S. S., & Mohamad, S. (2020). Production of cellulose nanofiber (CNF) from empty fruit bunch (EFB) via mechanical method. *Journal of Environmental Chemical Engineering*, *8*(1), 103024. https://doi.org/10.1016/j.jece.2019.103024

Suprihanti, A., Harianto, H., Sinaga, B. M., & Kustiari, R. (2018). Dinamika Konsumsi Rokok Dan Impor Tembakau Indonesia. *SEPA: Jurnal Sosial Ekonomi Pertanian Dan Agribisnis*, *14*(2), 183. https://doi.org/10.20961/sepa.v14i2.25016

Syafri, E., Jamaluddin, Sari, N. H., Mahardika, M., Amanda, P., & Ilyas, R. A. (2022). Isolation and characterization of cellulose nanofibers from Agave gigantea by chemical-mechanical treatment. *International Journal of Biological Macromolecules*, *200*, 25–33. https://doi.org/10.1016/j.ijbiomac.2021.12.111

Teixeira, R. F. A., McKenzie, H. S., Boyd, A. A., & Bon, S. A. F. (2011). Pickering emulsion polymerization using Laponite clay as stabilizer to prepare armored "soft" polymer latexes. *Macromolecules*, *44*(18), 7415–7422. https://doi.org/10.1021/ma201691u

Thomas, S. K., Begum, P. M. S., Midhun Dominic, C. D., Salim, N. V., Hameed, N., Rangappa, S. M., Siengchin, S., & Parameswaranpillai, J. (2021). Isolation and characterization of cellulose nanowhiskers from Acacia caesia plant. *Journal of Applied Polymer Science*, *138*(15), 1–9. https://doi.org/10.1002/app.50213

Tikekar, R. V., Pan, Y., & Nitin, N. (2013). Fate of curcumin encapsulated in silica nanoparticle stabilized Pickering emulsion during storage and simulated digestion. *Food Research International*, *51*(1), 370–377. https://doi.org/10.1016/j.foodres.2012.12.027

Valencia, L., Arumughan, V., Jalvo, B., Maria, H. J., Thomas, S., & Mathew, A. P. (2019). Nanolignocellulose extracted from environmentally undesired prosopis juliflora [Research-article]. *ACS Omega*, *4*(2), 4330–4338. https://doi.org/10.1021/acsomega.8b02685

Wang, H., Li, D., Yano, H., & Abe, K. (2014). Preparation of tough cellulose II nanofibers with high thermal stability from wood. *Cellulose*, *21*(3), 1505–1515. https://doi.org/10.1007/s10570-014-0222-6

Wang, J., Xu, J., Zhu, S., Wu, Q., Li, J. J., Gao, Y., Wang, B., Li, J. J., Gao, W., Zeng, J., & Chen, K. (2021). Preparation of nanocellulose in high yield via chemi-mechanical synergy. *Carbohydrate Polymers*, *251*(September 2020), 117094. https://doi.org/10.1016/j.carbpol.2020.117094

Wang, Q. Q., Zhu, J. Y., Gleisner, R., Kuster, T. A., Baxa, U., & McNeil, S. E. (2012). Morphological development of cellulose fibrils of a bleached eucalyptus pulp by mechanical fibrillation. *Cellulose*, *19*(5), 1631–1643. https://doi.org/10.1007/s10570-012-9745-x

WHO. (2017). *Tobacco and its environmental impact:*

an overview. https://doi.org/ISBN 978-92-4-151249-7

Yu, Z., Alsammarraie, F. K., Nayigiziki, F. X., Wang, W., Vardhanabhuti, B., Mustapha, A., & Lin, M. (2017). Effect and mechanism of cellulose nanofibrils on the active functions of biopolymer-based nanocomposite films. *Food Research International*, *99*, 166–172. https://doi.org/10.1016/j.foodres.2017.05.009

Zhai, W., Li, G., Yu, P., Yang, L., & Mao, L. (2013). Silver Phosphate/Carbon Nanotube-Stabilized Pickering Emulsion for Highly Efficient Photocatalysis. *Journal of Physical Chemistry C*, *117*(29), 15183–15191. https://doi.org/10.1021/jp404456a

Zheng, Y., Fu, Z., Li, D., & Wu, M. (2018). Effects of ball milling processes on the microstructure and rheological properties of microcrystalline cellulose as a sustainable polymer additive. *Materials*, *11*(7), 1–13. https://doi.org/10.3390/ma11071057